

[13]

Mechanism of Formation and Physical Classification of the Grown-In Microdefects in Semiconductor Silicon

V.I.Talanin^{1,a} and I.E.Talanin^{2,b}

¹Institute of State & Municipal Government, Zhukovskii Str. 70B,
69002 Zaporozhye, Ukraine

²State Engineering Academy, Lenin Avenue 226,
69006 Zaporozhye, Ukraine

^av.i.talanin@mail.ru, ^bi.e.talanin@mail.ru,

Keywords: Carbon, Carbon-Interstitial Aggregates, Classification, Grown-In Microdefects, Intrinsic Point Defects, Mechanism of Formation, Oxygen, Oxygen-Vacancy Aggregates

Abstract. This paper presents the scheme depicting the formation and transformation mechanism of the grown-in microdefects in FZ-Si and CZ-Si crystals as a function of a crystal growth rate. It is established and proved experimentally that concentrations of vacancies and self-interstitials at the crystallization front near the melting point are comparable, recombination of intrinsic point defects are hindered at high temperatures. Decomposition of the oversaturated solid-state solution of point defects during the silicon cooling below the crystallization temperature follows two independent mechanisms: vacancy-type and interstitial-type. The driving force of the defect formation is initial oxygen-vacancy agglomerates and carbon-interstitial agglomerates formed on impurities centers. At a certain thermal growth conditions the aggregation of point defects under vacancy-interstitial-type or interstitial type growth mode in the course of crystal cooling may cause the secondary defects occurrence around primary oxygen-vacancy and carbon-interstitial aggregates, namely vacancy microvoids and interstitial-type dislocation loops, accordingly. On the basis of experimental results the physical classification of the grown-in microdefects are proposed. The classification suggested follows from the heterogeneous formation and transformation mechanism of the grown-in microdefects.

Introduction

Achievements reached in the area of hyper pure silicon single crystals growing highlighted the further problem to study the peculiarities of the defect formation in such a perfect structure medium. It becomes of great importance now as microelectronics turned to megabit and gigabit integrated circuits fabricated by submicron-level technologies. Successful fabrication of high-quality single crystals and device structures with controlled and predictable parameters depends substantially on how a point defect ensemble is controlled.

The structure imperfections named as grown-in microdefects are formed during high-temperature growing and further cooling of dislocation-free single Si crystals. Presently, any local lattice imperfection from a few tens angstroms to few micrometers is deemed as grown-in microdefect. According to the generally accepted geometry (size) classification the grown-in microdefects belong to the transient class of defects between point and linear ones.

First data of etching pits in dislocation-free single Si crystals refer to the late sixties of last century [1]. A.J.R. de Kock introduced first classification for empty etching pits, having identified them as clusters. According to size of etching pits he divided clusters into two types: A-clusters (A-microdefects) and B-clusters (B-microdefects) [2, 3]. It should be noted that till the late seventies the grown-in microdefects have been studied in small-scale FZ-Si crystals (26 to 30 mm in diameter). It was established that A-microdefects observed in FZ-Si single crystals of 30 mm in diameter had a striated distribution at growth rate $V = 1$ to 3.5 mm/min and B-microdefects had a striated distribution at $V \leq 4.5$ mm/min [4]. When A-microdefects size increased up to a certain

limit (about 40 μm at $V = 1 \text{ mm/min}$), dislocations appear at single silicon crystals [5]. It was shown that fluctuation in temperature and presence of impurities (especially, carbon [6, 7] and oxygen [8, 9]) are basic factors responsible for the mechanism of A- and B-microdefects formation.

When crystals are grown at sufficiently high rates, a new type of microdefects was observed as uniform distribution and could be identified as dim regions after preferential etching and decoration [10]. These defects were classified as C- or D-microdefects depending on their macrodistribution images. Both types were visualized at the regions with uniform defect distribution of high density and, according to the authors of the paper [10], differed from each other by a distribution geometry. The uniform D-microdefects distribution is focused in the form of a "channel" in the central part of the crystal. Currently "C-microdefects" often referred to as "V-distribution" (or "V-band") and "W-distribution" (or "W-band"). However C-microdefects are also observed as rings or circles of irregular shape located at the most extensively cooled parts of the crystal. Therefore the term "C-microdefects" has a general meaning.

In small-scale silicon crystals grown by Czochralski method (CZ-Si) A-, B- and D-microdefects, identical to defects in FZ-Si, were also observed using preferential etching technique [11, 12]. Undoped or low-doped single crystals of 50 mm in diameter, which were grown at $V \leq 1 \text{ mm/min}$, contain A- and B-microdefects in a striated distribution. Furthermore, at $V \sim 1 \text{ mm/min}$ A- and B-microdefects are formed in concentrations comparable to their concentrations in silicon single crystals grown by floating-zone melting method. At rate of $V \geq 2 \text{ mm/min}$ the A- and B-microdefects generation is fully suppressed.

It should be noted that a discrepancy in classifying D-microdefects emerged. As stated above, first the term "D-microdefects" was introduced in 1977 by Sheikhet et al [10] for grown-in microdefects in FZ-Si ($V = 6 \text{ mm/min}$), which have uniform distribution in the form of a "channel" in the central part of the crystal. Quite possible, Roksnoer did not know of the paper [10] and in 1981 determined as D-microdefects such defects, which are generated also as uniform distribution in the form of a "channel" in the central part of the crystal FZ-Si (but at $V = 7$ to 8 mm/min) [13]. On the basis of X-ray topography results coupled with copper decoration, researchers in [13] made an assumption that the D-microdefects in FZ-Si are vacancy-type. It must be allowed for that in the theoretical model of the formation mechanism of microdefects in FZ-Si [14] Voronkov defines D-microdefects in accordance with classification [13]. The fact that uniform distribution of D-microdefects in the form of a "channel" in the central part of the crystal (in accordance with classification [10]) is not observed in CZ-Si makes the confusion in classification worse. Therefore, most authors still use a definition "D-microdefects" in accordance with [13]. Nevertheless, we believe that in the context of history and experimental results as for grown-in microdefects origin, such a definition of D-microdefects is erroneous.

What grounds are for such a conclusion? Later, using the transmission electron microscopy (TEM) we established that in FZ-Si crystals at $V = 6 \text{ mm/min}$ only interstitial-type defects are generated, while at $V = 7$ to 8 mm/min in FZ-Si crystals the interstitial-type and vacancy-type defects co-exist simultaneously [4, 15, 16]. Furthermore, we showed experimentally that at $V_{\text{crit}} \sim 6.5 \text{ mm/min}$ in accordance with ratio V/G (where V is a crystal growth rate; G is an axial temperature gradient) the mode of FZ-Si crystal growth is changing (from interstitial-type into vacancy-interstitial type and vice versa) [4, 15]. Thus, two quite different types of grown-in microdefects having uniform distribution were referred the same as to D-microdefects. Here we use the classification, which historically was first and more comprehensive [10]. Based on the classification [10] and TEM research results we define in this paper the grown-in microdefects in FZ-Si ($V = 7$ to 8 mm/min) having uniform distribution in the form of a "channel" in the central part of the crystal as "(I+V)-microdefects" [4, 15, 16].

New types of grown-in microdefects are observed in large-scale silicon crystals (over 100 mm in diameter). In particular, presently thermal oxidation typically leads to a ring-shaped distribution in

plane (111) of so-called “oxidation-induced stacking faults”, OSF-ring [17, 18]. Researches in a growth rate influence on a distribution of grown-in microdefects in single CZ-Si crystals of 150 mm in diameter revealed that OSF-ring is observed in crystals grown at a moderate growth rate (0.7 to 0.8 mm/min), and absent in crystals grown at growth rates 0.4 mm/min and 1.1 mm/min [19]. As is shown, stacking faults are formed around the plate-like oxygen precipitates [18]. When evaluating future trends in growing crystals of 300 mm and 400 mm in diameter [20], it should be noted that required growth rate decreasing (up to 0.55 mm/min for the crystal of 300 mm in diameter, which is twice less comparing to the crystal of 200 mm in diameter) below the critical rate in order to diminish the thermal stress in the crystal makes the task to fabricate ingots without OSF-ring rather complicated.

Outside OSF-ring the interstitial dislocation loops (A-microdefects) are observed [21, 22]. Inside OSF-ring there are defects, which according to observation techniques were named as FP-defects (flow pattern defects), COP-defects (crystal-originated particles) and LST-defects (light-scattering tomography defects) [23]. As is shown, all these defects are different forms of the same defect presentation obtained by various techniques, i.e. vacancy complexes, which are formed inside OSF-ring [24]. With the use of TEM the form and size of LST-defects were determined (100 to 300 nm) [25, 26]. Although TEM observation fails to determine the sign of the defect-induced lattice imperfection, on the basis of a smaller content of oxygen in the center of the defect as compared to the periphery and defect contrast image, was assumed that LST-defects constitute microvoids, i.e. they are vacancy-type. This enabled researchers to interpret all the defect types, identified by different techniques, as a one type of defects identical to D-microdefects in FZ-Si and CZ-Si, formed as a result of homogenous nucleation [25-28]. Unfortunately, these results strengthened the erroneous opinion among researchers that D-microdefects in FZ-Si and CZ-Si crystals are microvoids. It is generally assumed that depending on V/G ratio only interstitial-type dislocation loops (A-microdefects) or only microvoids (D-microdefects) are formed in large-diameter crystals. It is clear and simple approaches as in particular large microdefects either interstitial-type (A-microdefects) or vacancy-type (microvoids) considerably affect both electrophysical and mechanical properties of single-crystal silicon and discrete devices and integrated circuits. However, we believe such an approach is exceptionally technological because it does not allow for the physical nature of defect formation in the dislocation-free single crystal silicon.

There are several models of grown-in microdefects formation differing from each other both initial physical concept and level of validity. Every model is based on types and origin of dominating point defects in the growing crystal, which then are transformed into microdefects during cooling. Basic models of grown-in microdefects formation include the following: equilibrium interstitial-type model [7], non-equilibrium interstitial-type model [29], local melting model (drop model) [30], vacancy-type model [31], vacancy-interstitial type model [32, 33] and recombination-diffusion model [14, 27]. At present the recombination-diffusion model is the most well-grounded and optimal from the point of its quality. It is distinguished by compiling basics of other models. Furthermore, as many researchers acknowledged, it is convenient and plain to divide the grown-in microdefects simply to A-microdefects and microvoids on the basis of V/G ratio. The point is that V/G ratio allows correlating the lattice imperfection with the thermal growth conditions. Adjusting thermal growth conditions one can calculate the crystal defect structure. Voronkov's common model is based on the following: 1) there is a fast recombination between intrinsic point defects at temperatures close to melting point; 2) there are areas with only interstitial-type (A- and B-microdefects) or only vacancy-type microdefects (microvoids or D-microdefects); 3) there is a critical parameter $C_{crit} = V/G$. When $V/G < C_{crit}$, self-interstitial atoms dominate in the crystal (interstitial-type crystal growth) and when $V/G > C_{crit}$, vacancies prevail in the crystal (vacancy-type crystal growth). The effect of V/G ratio is reversible and repeatable: reduce V/G – and find A-microdefects and no microvoids; increase V/G – and find microvoids and no A-

microdefects. To apply this criterion one should measure or calculate the value of G . However this model does not allow for the affect of impurities (except for oxygen) and does not reflect a real physical nature of formation processes of the grown-in microdefects in silicon single crystals. Recently, Voronkov reported he took into consideration the other impurities in addition to oxygen, which effect the formation of microdefects [34]. He suggested that V/G ratio is shifted by impurities. Some impurities, such as oxygen, nitrogen, and hydrogen, trap vacancies and cause a downward shift in the critical V/G ratio (and also a fast increase in the fraction of trapped vacancies). Other impurities, like carbon, trap self-interstitial, and cause an upward shift in the critical V/G ratio (and also an increase in the fraction of impurity interstitials) [34].

The drawbacks of the existing classification (and the drawbacks of the theoretical models based upon it) are in that it does not provide any information about the sign of lattice imperfection, which depends on the microdefect type. The sign of defect-induced lattice imperfection (often defined as the microdefect origin) bears an implicit information of the defect chemical composition. At the same time it allows to determine the mechanisms, through which the grown-in microdefects form and transform. It was exactly the absence of this parameter that caused confusion in identification and classification of D-microdefects in FZ-Si and CZ-Si.

1 Experimental

The comprehensive study aiming to reveal the mechanism of the grown-in microdefects formation and transformation is required to solve the problem of the defect formation in dislocation-free single crystal silicon. Following this way, we have been researching the distribution images and images of individual properties (size, form, sign of lattice imperfection) of grown-in microdefects in FZ-Si and CZ-Si crystals, which were grown at different thermal conditions. Special attention was drawn to study the FZ-Si crystals, which are hyper pure crystals (most of them have contents of oxygen and carbon less than $5 \cdot 10^{15} \text{ cm}^{-3}$). The principal objective of study was to distinguish the operative body (basis) of the mechanism of the grown-in microdefects formation, effecting which (i.e. changing in thermal growth conditions, doping, thermal processing) one can control the process of defect formation in the dislocation-free single crystal silicon.

We have conducted a series of experiments with the FZ-Si and CZ-Si using preferential etching and transmission electron microscopy. The silicon crystals of 30 mm (FZ-Si) and 50 mm (CZ-Si) in diameter were studied. These diameters were chosen because all the known types of the grown-in microdefects are formed in crystals of such diameters when thermal conditions of crystal growth vary. FZ-Si crystals were not doped, oxygen and carbon concentrations were less than $5 \cdot 10^{15} \text{ cm}^{-3}$, the number of passes varied from 2 to 10, $\rho = (2 \dots 4) \cdot 10^3 \text{ } \Omega \cdot \text{cm}$. Concentration of the electrically active impurities were less than 10^{12} cm^{-3} . CZ-Si n-type crystals were with $\rho = 10 \dots 50 \text{ } \Omega \cdot \text{cm}$, oxygen concentration $\sim (4 \dots 7) \cdot 10^{17} \text{ cm}^{-3}$, carbon $\sim (5 \dots 7) \cdot 10^{16} \text{ cm}^{-3}$. The crystals were grown at constant growth rates ranging from 1 to 9 mm/min (for FZ-Si) and 0.5 to 3 mm/min (for CZ-Si). Several crystals were obtained under specially programmed growth rate change. To freeze-in the initial stages of formation of grown-in microdefects we conducted quenching of crystals.

Sirtl etch was used to identify microdefects of different types and their distribution images. The inside-outside contrast method, black-white contrast method and defocused dark-field image method (2.5D) were used to determine the sign of lattice imperfection. Electron microscope with 100 kV acceleration voltage was employed that excludes radiation defect infusion [35, 36]. To avoid contamination of the surface by alkali atoms and hydrogen (which are known to penetrate while etching to a depth of several micrometers), the samples for the TEM study were not subjected to that procedure. Knowing the etch pattern for a certain silicon wafer, one can rather exactly cut the samples for the TEM study from a selected place of a near-by wafer, thus the identity of microdefects distribution over the cross-section of both wafers being ensured.

2 Results

2.1. Scheme formation and transformation mechanism of grown-in microdefects in silicon single crystals. Large number of crystals studied (more 60 ingots FZ-Si and more 20 ingots CZ-Si), which were obtained under various thermal growth conditions, enabled us to make a schematic representation of the microdefect distribution in FZ-Si and CZ-Si under the changing crystal growth rate (Fig.1).

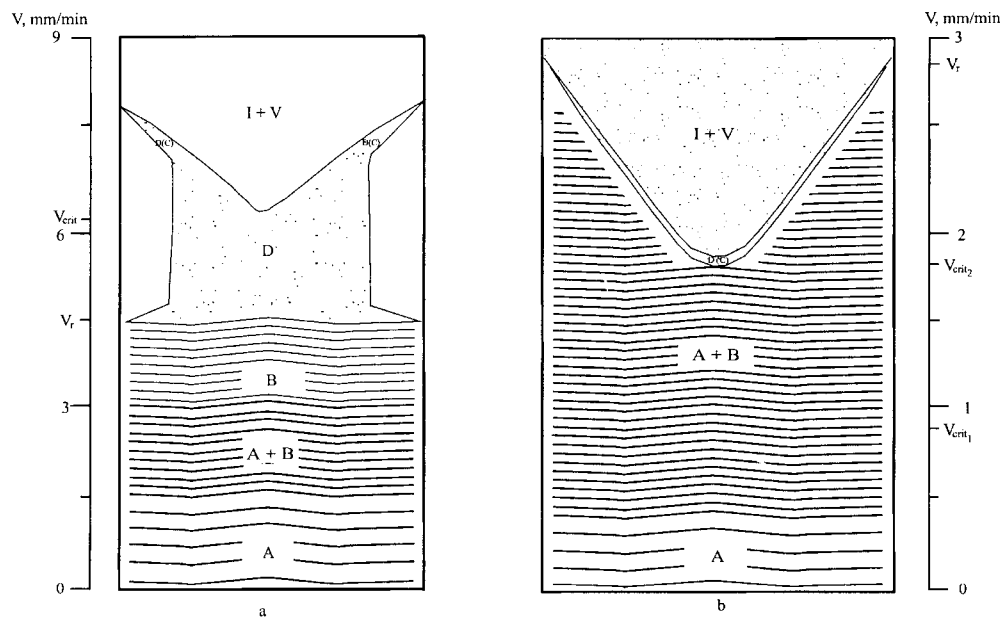


Fig 1. Schematic formation and transformation mechanism of microdefects in silicon single crystals, plane (112): a – FZ-Si crystal Ø 30 mm; b – CZ-Si crystal Ø 50 mm; V_{crit} , $V_{crit 2}$ – crystal growth rates defined experimentally, at which the vacancy-type microdefects appear (disappear), mm/min; V_r – crystal growth rate, at which the remelting phenomenon is suppressed; $V_{crit 1}$ – crystal growth rate calculated theoretically, at which vacancy-type microdefects appear while the interstitial-type defects disappear (according to Voronkov's model), mm/min.

As one can see in Fig.1a, with gradual increase of growth rate, one type of microdefects in FZ-Si crystals is replaced progressively with the other type. A-microdefect large swirls are replaced with smaller swirls of B-microdefects. After the rate V_r reaches a certain value (at which the remelting phenomenon is suppressed) B-microdefects are replaced with uniform D-microdefects distribution. For FZ-Si we determined the adjusted value of rate V_r to be ~ 4.5 mm/min. Our study results showed that above a certain critical growth rate V_{crit} the (I+V)-microdefects (defect-free region on Fig.1a) begin to appear in crystals, while before V_{crit} only D-microdefects could be detected. If $V > V_r$, D-microdefects usually converge in a channel, which afterwards at $V \geq V_{crit}$ begins to diverge towards the periphery of the crystal (C-microdefects in accordance with classification [10]). If the crystal growth rate continues to rise, the ring size diminishes (in plane (111)), and at $V \sim 8$ mm/min the ring of D(C)-microdefects disappears. Fig.2a and Fig.2c shows the difference between the images of FZ-Si crystals selective etching at $V = 6$ mm/min (D-microdefects) and at $V = 8$ mm/min

((I+V)-microdefects). Thus, as the crystal growth rate decreases, the grown-in microdefects are continuously transformed.

As for SZ-Si crystals growing, the growth rates are moved to smaller values. The appearance of uniform defect distribution is typical for the values: $1.5 \text{ mm/min} < V < 2 \text{ mm/min}$. Though, according to Voronkov's model, interstitial-type A- and B-swirls should appear only at $V < V_{\text{crit } 1}$, where $V_{\text{crit } 1}$ is defined as a theoretical value characterised by the vacancy-type microdefects appearance and the interstitial-type microdefects disappearance [14, 27]. Data in Fig.1b makes it clear that D-microdefects are not detected in CZ-Si in channel distribution. This may be concerned with the following. The change in thermal growth conditions causes the suppression of remelting phenomenon (this phenomenon is responsible for striated distribution of A- and B-microdefects) that appears in FZ-Si at interstitial-type growth (i.e. at $V_r < V_{\text{crit}}$) and in CZ-Si at vacancy-interstitial-type growth (i.e. at $V_r > V_{\text{crit}}$). Furthermore, oxygen and carbon are present in CZ-Si crystal in much greater concentrations than in FZ-Si. Therefore, oxygen precipitation is in close interrelation with the CZ-Si defect structure and leads to interstitial-type dislocation loops (A-microdefects) appearance outside the D(C)-microdefects distribution (i.e. outside the D(C)-microdefects ring in plane (111)).

Consequently, as the crystal growth rate increases, the crystallisation front curvature decreases, thus conducing to that the plane (111) emerges to the crystallisation front and the channel and ring distribution of D-microdefects are formed. This process proves the heterogeneous nature of microdefect generation. Decreasing the crystallisation front curvature results in the temperature gradient reducing. However, in its turn, the axial temperature gradient is not constant through the entire crystal diameter. Thus, $C_{\text{crit}} = V/G(r)$ (where $G(r)$ generally increases from the crystal center to its edge) [37], that leads to generating V-shaped distribution of D(C)-microdefects in plane (112).

Growth rate values, at which the ring-shaped distribution in plane (111) of D(C)-microdefects is observed, range within 1 to 2 mm/min for CZ-Si crystals of 80 mm in diameter and within ~ 0.5 to 0.8 mm/min for CZ-Si crystals of 300 mm in diameter [20]. The ring-shaped distribution of D(C)-microdefects can be defined as ring OSF-defects after thermal processing. Ravi suggested [38], that microprecipitates SiO_2 as well as microprecipitates SiC are responsible for generation of stacking faults.

We regard the defects within the area of ring-shaped distribution as ones similar to D(C)-microdefects in FZ-Si crystals. Therefore, varying the thermal growth conditions results in that D(C)-microdefects in CZ-Si crystals are observed only in the ring-shaped distribution. The ring-shaped uniform distribution of D(C)-microdefects serves as the boundary between the interstitial microdefects area in the striated distribution (A-microdefects) and (I+V)-microdefects. Ring-shaped distribution of D(C)-microdefects is formed as a result of Si crystal thermal growth conditions and after the plane (111) is transposed to the crystallization front (edge effect). V-type distribution of D(C)-microdefects in plane (112) is the experimental representation of V/G ratio. Obtained experimental results allow suggesting that the defect formation mechanism (and classification of the grown-in microdefects) in FZ-Si is identical to that in CZ-Si.

2.2. Quenched crystals study. It is essential to study initial stages of defect formation in order to determine the mechanism of grown-in microdefects formation and transformation. With this purpose the FZ-Si single crystals grown at various growth rates (2.0, 3.0, 6.0, 9.0 mm/min) were subjected to quenching. One of most effective crystal quenching methods was applied, namely melting zone decantation, when at a certain moment a zone is blown with the directed argon flow. The temperature of grown-in microdefects was determined experimentally and by theoretical calculation. Neimark et al [39] measured thermal fields, which take place during growth of silicon single crystals, by the thermocouple. They suggested the following empirical formula to describe the dependence of an axial temperature gradient on the growth rate of crystal:

$$dT/dL = 10 + (L - 16)^2 \cdot \exp(-61.2V - 0.28), \quad (1)$$

where L is a distance from crystallization front, cm; V is a crystal growth rate, cm/s. The experimental values well coincide with values calculated from (1). The error between the calculations from (1) and experimental values does not exceed $\pm 2\%$. Our experiments allowed defining the temperatures of grown-in microdefects formation.

Table. The temperature of grown-in microdefects formation

Rate of growth, mm/min	Conditions of treatment	Type of grown-in microdefects	Distance from the front of crystallization, mm	Temperature of formation, ± 20 K
2.0	Quenching	A	23	$T_A = 1373$
3.0	Quenching	B	-	$T_B = 1653$
6.0	Quenching	D	26	$T_D = 1423$
6.0, 9.0	Quenching	I+V	-	$T_{I+V} = 1653$

When studying a detachment surface, we established that microdefects have been not detected directly at the crystallization front because of introducing dislocations due to a thermal impact [4]. Therefore it is hard to define the exact starting moment of the formation process of B- and (I+V)-microdefects. Although we can assume that at the given growth conditions the B- and (I+V)-microdefects are formed as soon as cooling starts due to complexation of silicon interstitial atoms, vacancies and impurity atoms. Distance from the front of crystallization, where the dislocations are observed, is not more 1 to 3 mm and theoretically tends to zero. Experiments in crystal quenching demonstrate that the (I+V)-microdefects are first to appear near the crystallization front and then during the cooling the D(C)-microdefects, B-microdefects and A-microdefects are formed. It is worth to note that CZ-Si and FZ-Si crystals thermal processing also gives rise to transformation of interstitial-type microdefects in direction as follows: D(C)-microdefects \rightarrow B-microdefects \rightarrow A-microdefects [16, 40].

When quenching the FZ-Si crystals grown at $V = 6$ mm/min, the so-called defect-free area between the crystallization front and D-microdefects area is generated. The TEM study imaged this defect-free area as black-white spots (similar to Fig.2d). Such a contrast is known to be caused by dynamic conditions of electron reflection from crystallographic planes near the defect. In the thin parts of samples these defects are imaged as black spots for kinematic conditions of electron reflection. It should be noted that kinematic images of defects are more useful for the evaluation of the size of these defects. For the majority of the observed defects it is 3 to 7 nm. The concentration of defects found by electron microscopy is $\sim 4.5 \cdot 10^{13} \text{ cm}^{-3}$. The view of defect images did not yet allow defining the geometric shape of these defects. To state the physical nature of the observed microdefects (the sign of the imperfection around it), their black-white contrast with all the peculiarities of their behaviour has been investigated in dependence on the depth of the microdefect position in thin crystals [41]. For an unambiguous identification of observed defects the method 2.5D has been applied (observation of stereocouples of underfocused and overfocused images) [42]. These methods reveal that the defect-free area contains interstitial-type and vacancy-type defects. Defects have similar image contrast, but vacancy defects on the whole are somewhat greater in size than defects of interstitial type. It should be noted that area with D-microdefects contains only interstitial-type defects a half as large again that size of (I+V)-microdefects, while the concentration of D-microdefects is three times less than the concentration of (I+V)-microdefects.

In addition, with use of TEM study made for FZ-Si crystals grown at $V = 9$ mm/min and then quenched, the interstitial-type and vacancy-type microdefects have been revealed near the crystallization front in concentrations comparable with each other. Thus, defect-free areas near the

crystallization front indeed contain defects of both deformation types, which should be interpreted as quite new and rather substantial fact. Furthermore, it makes clear from these experiments why we introduce the term "(I+V)-microdefects" into the classification of grown-in microdefects.

Experimental results obtained in the quenched crystals study demonstrate that the recombination process of intrinsic point defects near the crystallization front is hindered due to the recombination barrier. Microscopic model of such a barrier was developed in detail in papers by Gosele [43-45]. The root of model lies in that the configuration of intrinsic point defects at high temperatures defines the barrier's dependence on temperature. As is assumed within the model's framework, at high temperatures the self-interstitials and vacancies are extended through several atomic volumes (11 atoms occupies 10 cells), i.e. there is a disordered area around the point defect, which is isotropic-extended up to the atoms of the second coordination sphere. Recombination only occurs if both defects are simultaneously contracted all-around the same atomic volume. As the extended defect configurations have more microstates than the point defect, such a contraction reduces entropy and, consequently, an entropy barrier $\Delta S < 0$ exists. As temperature is lowering, the barrier decreases and disappears at low temperatures at all and defects recombine easily. This is connected with changing in configuration of intrinsic point defects, which are extended at high temperatures and have a point-like dumbbell shaped configuration at low temperatures, as shown in [45, 46]. It should be emphasized that a theory of extended defect configurations as well as the theory of recombination barrier has been acknowledged in a number of up-to date papers [47-50].

Taking into consideration the available dynamic equilibrium between the vacancies and intrinsic points of silicon atoms as a result of competition between the recombination and continuous thermal generation of Frenkel pairs and considering the local equilibrium

$$C_I C_V = C_I^{eqv} C_V^{eqv}, \quad (2)$$

which is established regardless the generating technique of the concentration ratio of vacancies (C_V) to intrinsic interstitial atoms (C_I), where C_I^{eqv} is an equilibrium concentration of intrinsic interstitial atoms, C_V^{eqv} is an equilibrium concentration of vacancies, accordingly, then the time required to reach equilibrium provided there is no recombination barrier may be determined by:

$$\tau \leq \frac{\Omega}{4\pi D^S r_0}, \quad (3)$$

where Ω is a volume cell; D^S is a self-diffusion coefficient; r_0 is an effective recombination cross-section [14]. Assuming that the recombination is defined not only by diffusion but also by height of the recombination barrier, which exceeds free diffusion energy on the value of

$$\Delta G = \Delta H - T\Delta S, \quad (4)$$

as well as that the recombination barrier is defined by the entropy component of the expression (4) and applying the concept of extended defect configurations for entropy barrier microscopic model [45], we obtained the barrier value at $T = 1685$ K (the crystallization temperature), which is $\Delta G = 1.674$ eV [4]. Then, we can estimate τ value from (3) allowing for existing recombination barrier:

$$\tau = \frac{\Omega}{4\pi D^S r_0 \cdot \exp(-\Delta G/kT)} \quad (5)$$

With regard to ΔG value, we obtain $\tau \approx 53$ min. Therefore the recombination does not get through when standard silicon ingots and standard time of its growth are taken. Such discrepancies may be explained as follows. The Voronkov's model, firstly, assumes the theory of enthalpy barrier and, secondly, denies the fact that intrinsic point defects of both types co-exist simultaneously. Besides, according to Voronkov's model τ is determined individually for interstitial-type and vacancy-type growth modes proposed by him, without taking into consideration the coefficient of vacancy and intrinsic interstitials joint self-diffusion. Experimentally obtained results, proving the

co-existence of vacancy-type and interstitial-type microdefects and, consequently, occurrence of both types of intrinsic point defects near the crystallization front, may be only explained within the framework of theory, which allows for such a fact and theory of entropy barrier.

Since at temperatures close to the melting temperature the equilibrium concentrations of vacancies and self-interstitial atoms co-exist simultaneously in dislocation-free silicon single-crystals, the oversaturated solid-state solution of intrinsic point defects has been decomposing concurrently at two mechanisms: vacancy-type and interstitial-type. Depending on growth conditions (in particular, on the V/G ratio) the silicon crystals grow under the vacancy-interstitial and interstitial growth modes. This definition of crystal growth modes is concerned with the nature of grown-in microdefects.

2.3. Physical nature of the grown-in microdefects. TEM study of FZ-Si and CZ-Si crystals grown at accelerated growth rates gave us a possibility to define the physical nature of (I+V)-microdefects, D-microdefects and C-microdefects (see Fig.1). We were first who observed these defects in FZ-Si [15]. Fig.2 shows the typical images of (I+V)-microdefects and D-microdefects (after selective etching and TEM images).

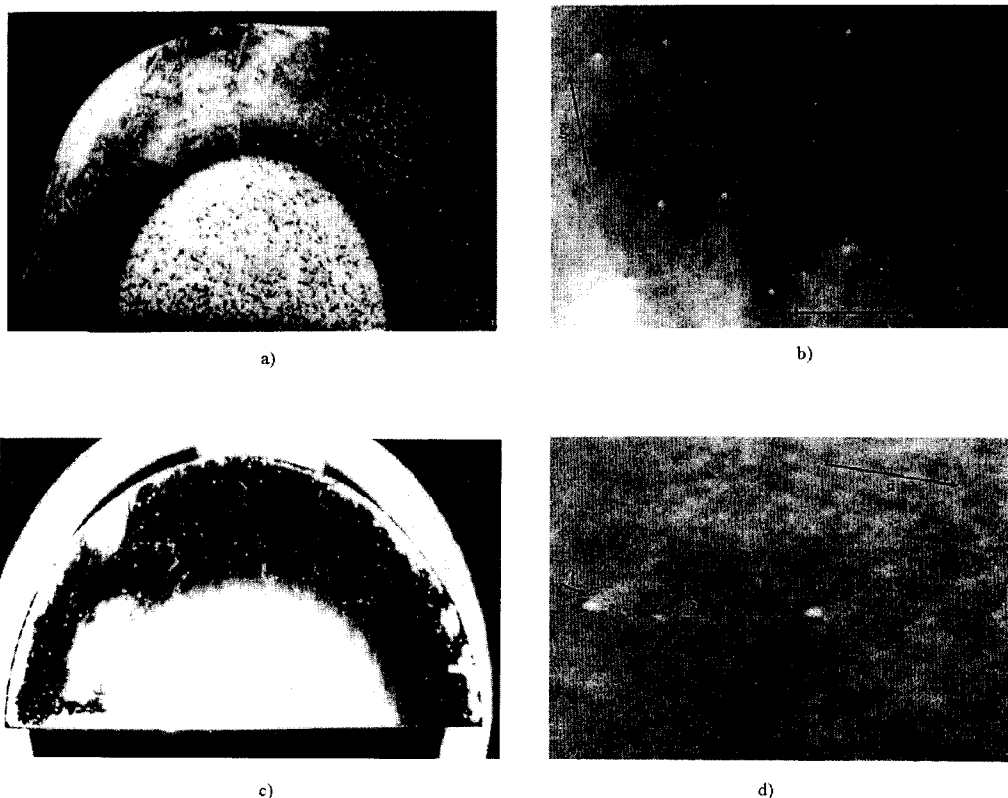


Fig.2. D-microdefects and (I+V)-microdefects in FZ-Si: a) D-microdefects ($V = 6$ mm/min), selective etching, plane (111); b) D-microdefects, TEM, $\bar{g} = (\bar{2}20)$, dark field, $s = 0$; c) (I+V)-microdefects ($V = 8$ mm/min), selective etching, plane (111); d) (I+V)-microdefects (1 – V-defects, 2 – I-defects), TEM, $\bar{g} = (\bar{2}20)$, dark field, $s = 0$.

TEM study was performed similar to above mentioned in section 2.2. We investigated more than 1000 specimens to establish the statistical relevance of our results. We carried out the TEM study on electronic microscope with accelerating voltage 100 kV, thus excluding the introduction of radiation defects. As the strain field around the defect exceeds the defect size, the shape of the defect is not visible. Main results for FZ-Si [4, 15]:

- D-microdefects constitute clusters of interstitial-type point defects with size of 4 to 10 nm; they may be considered as uniform B-microdefect distribution;
- C-microdefects are entirely identical to D-microdefects as contrast of TEM images and the sign of lattice imperfection is concerned; they only differ by the distribution geometry. Therefore, there is no need to separate them into a distinct type;
- At high growth rates (exceeding 6 mm/min), the interstitial-type microdefects occur simultaneously with the vacancy-type microdefects and localize themselves in the same areas – (I+V)-microdefects.

Evaluation of quantitative ratio for vacancy to interstitial-type defects gave us a value $\sim 1:4$ (at $V = 7.5$ mm/min). When accelerating the crystal growth, the share of vacancy-type microdefects increases in total number of defects. It is established in crystals with D-microdefects that the growth rate accelerating gives diminishing in defect sizes.

When CZ-Si 50-mm crystals are grown at a changing growth rate, an area of uniform defect distribution are formed at $V > 2$ mm/min with its increase in diameter as the growth rate is raising (Fig.3a).

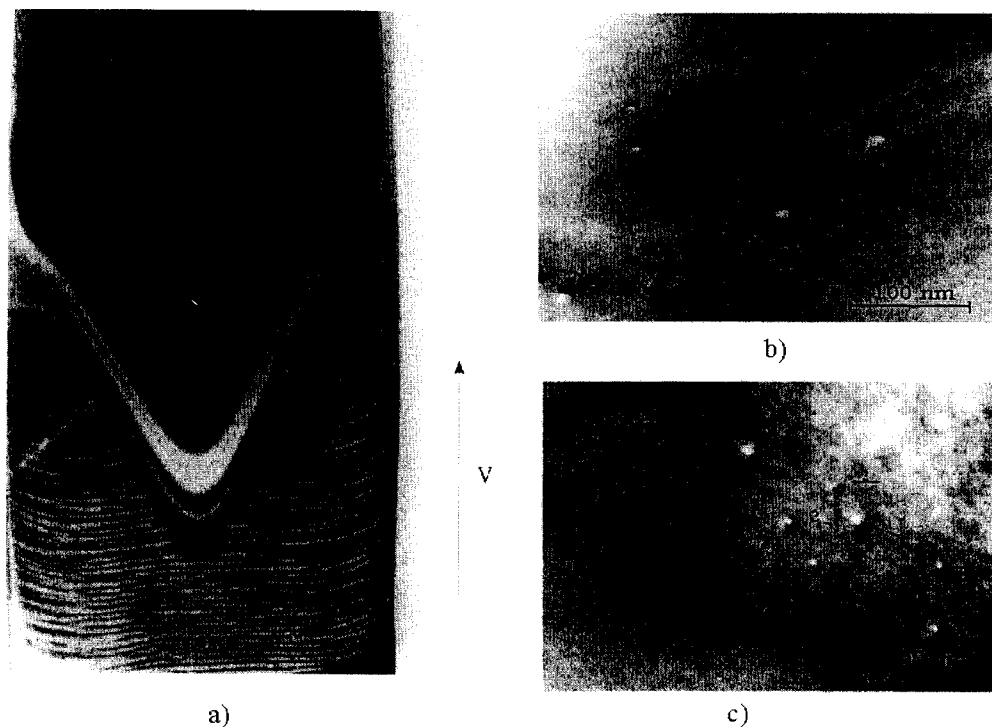


Fig.3. D(C)-microdefects and (I+V)-microdefects in CZ-Si ($V = 1.8 \dots 2.8$ mm/min): a) selective etching, plane (112); b) D(C)-microdefects, TEM, $\bar{g} = (\bar{2}20)$, dark field, $s = 0$; c) (I+V)-microdefects (1 – V-defects, 2 – I-defects), TEM, $\bar{g} = (\bar{2}20)$, dark field, $s = 0$.

Quite often preferential etching does not reveal the defects in the center of the crystal. However, in this case, the central region is surrounded by high-density uniform defect distribution. According to classification [10] and researches presented in [11, 12], we identified these defects as D(C)-microdefects that correspond to D-microdefects in FZ-Si. In plane (111) one can observe a ring of D(C)-microdefects containing so-called "defect-free" area inside. It will be observed that this ring of defects is often called OSF-ring in publications. But "oxidation-induced stacking faults" do not pertain to grown-in microdefects, because they occur after different thermal treatment procedures [17]. As the growth rate increases, the ring of D-microdefects moves to the crystal periphery while the "defect-free" area inside the ring increases in diameter. At $V = 3$ mm/min the ring of D-microdefects disappears completely.

We conducted TEM directly within the ring of D(C)-microdefects and inside this ring (in the "defect-free" area). Within the ring of D(C)-microdefects we observed black-white contrast defects. Their concentration was 10^{13} to 10^{14} cm⁻³, and their size was 4 to 12 nm. A. Bourret [8] was first who observed these defects in CZ-Si, however the sign of lattice imperfection has not been determined yet. By black-white and 2.5D methods we determined that these defects only induce interstitial-type CZ-Si lattice strain. In defect-free area inside the ring of D(C)-microdefects we observed defects of the same size and concentration. The contrast analysis of TEM-images showed both vacancy-type and interstitial-type defects. TEM-observation of CZ-Si grown at $V = 3$ mm/min also prove the coexistence of both vacancy-type and interstitial-type microdefects. Obtained experimental results are consistent with experimental results for FZ-Si [4]. We analyzed the white-black contrast of D(C)-microdefects image at dynamic imaging conditions. Such analysis helps to define the crystallographic properties of these defects [51]. Inclusions, dislocations dipoles, dislocation loops may be characterized as small-size lattice imperfections with localized strain fields [41, 52]. The contrast analysis proved that D(C)-microdefects may be theoretically considered as dislocation loops with Burgers vector $\bar{b} = 1/2[100]$ and $\bar{b} = 1/2[110]$. Planes $\{100\}$, $\{110\}$, $\{111\}$ can be possible planes of dislocation loops occurrence [4].

These experimental results were obtained with use of TEM for the case of amplitude contrast by means of analyzing the diffraction image with black-white imaging contrast and 2.5D techniques. However, these techniques have certain weaknesses and restrictions, related both to uncertain depth of defect occurrence and to especially small size of defects being investigated. That is why D-microdefects study using the independent TEM technique by the lattice direct resolution [15] is of great value. Being armed with this method based on phase contrast and giving the lattice image of ~ 0.2 nm resolution, we obtained detailed information of D-microdefects fine structure. We have been studying n-type undoped FZ-Si single-crystals with $\rho = 2000$ Ω ·cm, which were vacuum-grown at $V = 6$ mm/min. Oxygen and carbon concentration was determined by infrared absorption spectrum and amounted to: $< 1 \cdot 10^{16}$ cm⁻³ for oxygen and $1.6 \cdot 10^{16}$ cm⁻³ for carbon. Authors [15, 53] observed the D-microdefects electron-microscopic images of two types: having regular (periodic) and irregular (amorphous) structure (Fig. 4). Microprecipitates of SiO₂ amorphous phase produce the amorphous image [53]. From our point of view, the regular structure belongs to SiC microprecipitates. Both types of D-microdefects revealed are of interstitial-type. Hence, two independent TEM study techniques (amplitude contrast and direct lattice resolution) established the interstitial nature of D-microdefects while being of two types in the crystal.

TEM studies of crystals with B-microdefects (FZ-Si, $V = 4$ mm/min) showed the same defects of white-black contrast of image as for the crystals with D-microdefects. However, B-microdefects size ranges within 15 to 50 nm, having concentration $\sim 10^{10}$ cm⁻³. Zero contrast line is often displayed as broken line. The white-black contrast imaging and 2.5D methods were used to define the physical nature of B-microdefects. We established that all these defects induce the compressive strain in the crystal, i.e. they are of interstitial type [4, 16]. Geometry of a certain part of B-microdefects emerged under conditions deviating from dynamic image. In this case B-microdefects

look like plates having at planes $\{111\}$ projection a square and diamond shapes (Fig.5b). Either diamond diagonal lines or square sides are

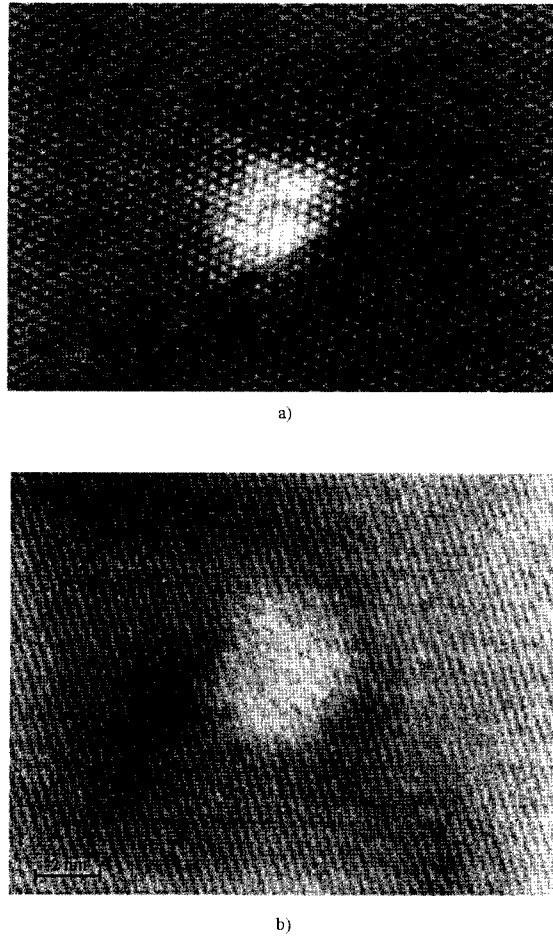


Fig.4. D-microdefects in FZ-Si ($V = 6$ mm/min), TEM (direct solution of crystalline lattice): a) recurring structure; b) amorphous structure.

parallel to the diffraction vector $\bar{g} = (220)$. Hence, such defects have cuts in directions $[100]$ or $[110]$ and lie in planes $\{100\}$.

It should be noted that the agglomerations in planes $\{100\}$ with cuts along the directions $[110]$ have been observed in CZ-Si crystals and identified as SiO_2 precipitates [8, 54]. This agglomerates has an amorphous structure and they represent SiO_2 amorphous phase [8, 15]. They may be considered as a model of edge dislocation interstitial loops with Burgers vector $\bar{b} = 1/2[100]$ [8]. The generation and growth of such agglomerations caused by the oxygen precipitation induce the strong compression of silicon lattice. Relieving from compression results in the prismatic extruding of the interstitial-type dislocation loops (A-microdefects) [4, 55]. Furthermore, SiO_2 precipitates growing causes the oversaturation of solid-state solution of silicon intrinsic interstitials and leads to A-microdefects occurrence [4, 7, 56, 57]. Hence, A-microdefects generation is associated with the

generation and growth of precipitates (i.e. primary grown-in microdefects). Our TEM studies prove that (I+V)-microdefects, D(C)-microdefects and B-microdefects should be referred to as the primary grown-in microdefects. Besides, two forms of D(C)-microdefects existence and size nearness and similar contrast of electron-microscopic images enable us to presume they are uniform distributed small-size B-microdefects.

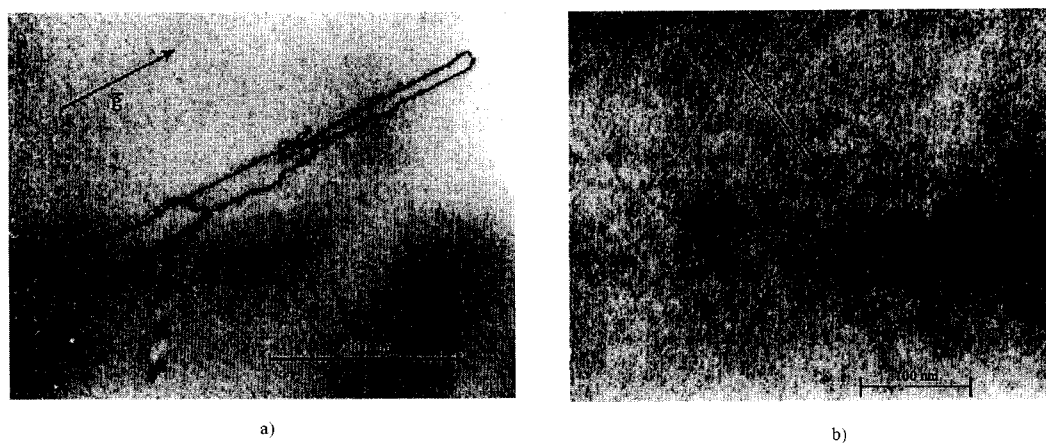


Fig. 5. A-microdefects and B-microdefects in FZ-Si: a) A-microdefects, TEM, $\bar{g} = (0\bar{2}2)$, light field, $s < 0$; b) B-microdefects, TEM, $\bar{g} = (\bar{2}02)$, dark field, $s > 0$.

TEM studies of crystals with A-microdefects (FZ-Si, $V = 2$ mm/min) were carried out with the use of electronic microscope JEM-1000 [58]. A-microdefects physical nature has been analyzed by the inside-outside contrast method [59]. The dislocation interstitial loops with Burgers vector $\bar{b} = 1/2[110]$ were revealed lying in planes $\{110\}$ and $\{111\}$ (Fig.5a). The loop size increases as the crystal growth rate slows down. In some cases dislocation lines of loops were decorated with residual oxygen and carbon impurities. These experiments quite well match the earlier obtained results of A-microdefects study [29, 57]. It should be pointed to that it was recently shown the A-microdefects in CZ-Si crystals are also interstitial type dislocation loops [21, 60]. As is reported, the vacancy microvoids were not observed in small-scale FZ-Si and CZ-Si crystals.

Our experimental results in studying the physical nature of grown-in microdefects illustrate the entire interrelation of their generation and further growth with the presence of carbon and oxygen impurities in the silicon crystal. It is worth to emphasize, this interrelation is revealed experimentally in hyper pure undoped silicon single crystals, where carbon and oxygen concentration is less than $5 \cdot 10^{15} \text{ cm}^{-3}$. So, the study of so-called "oxygen-free" FZ-Si crystals is of much importance. A background oxygen impurity is an important factor influencing the formation mechanism of the grown-in microdefects. And a carbon background impurity is as important as above, especially for FZ-Si [4, 16]. For instance, we showed in CZ-Si that the points with maximum carbon concentration and the points with maximum density of microdefects coincide [40]. However, if microdefects concentration is considered as a function of carbon concentration in different CZ-Si crystals, the relationship will be a bit different. Then, as carbon content increases to $5 \cdot 10^{16} \text{ cm}^{-3}$, the concentration of the grown-in microdefects oscillates. When carbon concentration exceeds $5 \cdot 10^{16} \text{ cm}^{-3}$, the concentration of microdefects tends to rise as carbon concentration rises. Apparently, when carbon concentration is below $5 \cdot 10^{16} \text{ cm}^{-3}$, oxygen impurities are more important

in the formation of microdefects. After doping by oxygen from a gas phase, D-microdefects are formed and concentration of B-microdefects is increased [16].

Comparing FZ-Si crystals with CZ-Si crystals one can see the changes in distribution images of grown-in microdefects. This is related to both the change in thermal growth conditions of the crystal and a much greater concentration of carbon and oxygen impurities (with the latter being especially important). However the formation mechanism of the grown-in microdefects in CZ-Si will allow two independent directions in which the supersaturated solid solution of the point defects is relaxed. The study of the nature of the grown-in microdefects in CZ-Si proves that the processes responsible for their formation are similar to those in FZ-Si.

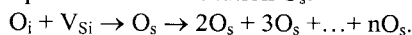
So, the recombination process of intrinsic point defects in FZ-Si and CZ-Si single-crystals near the crystallization front is hindered due to the recombination barrier. Vacancies and self-interstitials find out drains in the form of background oxygen and carbon impurities. Consequently, in the context of physical nature of defect formation in real small-scale crystals the Voronkov's theoretical model fails to be consistent. Considering a concept of entropy barrier and a factor of simultaneous self-diffusion of vacancies and self-interstitials [45], we may reason in this way contrary to the theory of Voronkov that there is a recombination barrier [4]. Experimental results of TEM studies and heterogeneous formation mechanism of the grown-in microdefects prove the theoretical considerations of Hu, Sirtl [32, 33] and Gosele [45] to be true.

3 Discussion

3.1. Formation mechanism of the grown-in microdefects. From our point of view the experiments with hyper pure FZ-Si are of especial importance. It was these experiments that allowed us to suggest the heterogeneous formation mechanism of the grown-in microdefects [4]. Its basic principles can be outlined as follows:

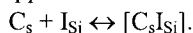
- recombination of intrinsic point defects at crystallization temperature is hindered because of recombination barrier;
- background impurities of oxygen and carbon participate in the process of defect formation as nucleation centers, and consequently participate in the processes of further growth and transformation of grown-in microdefects;
- cooling-induced decomposition of the oversaturated solid solution of point defects in silicon follows two mechanisms: vacancy-type and interstitial-type.

For the vacancy mechanism theoretically only vacancy aggregation and joint vacancy-impurity aggregation are possible. Vacancy-impurity aggregation begins earlier than a vacancy aggregation. Interstitial atoms of oxygen are very mobile, and therefore the formation of complexes is stimulated by leaving interstitial oxygen in positions of substitution O_s :

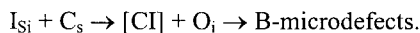


At lower temperature, O_s can be formation centers of microprecipitates of oxygen. When microprecipitates are formed, there is a surplus of volume and one vacancy will be consumed by a growing precipitate for each two oxygen atoms precipitated. The absorption of vacancies and impurities by growing microdefects results in a decreased concentration of vacancies in comparison with oxygen concentration. As a result precipitates begin to absorb oxygen without participation of vacancies, their sizes are increased and then the type of a strain around them varies from vacancy (tensile) to interstitial (compressive). The full transition boundary can be determined from the relation V/G . Thus, the parameter C_{crit} does not describe a change in condition of growth mode (interstitial or vacancy). This parameter describes conditions of the vanishing (emerging) of microdefects of a vacancy type as a result of diffusion and interaction of point defects during cooling of the crystal.

The centers of nucleation in a base of interstitial atoms of oxygen exist also for the interstitial mechanism. However, here a catalytic role is played by carbon atoms. The oversaturation of interstitial atoms of silicon results in the appearance of complexes $[C_s I_{Si}]$:



The decrease of the critical radius $[C_s I_{Si}]$ nuclei and the acceleration of a diffusion C_s occur here. Thus, agglomerates $[C_s I_{Si}]$ are formed. Furthermore, during supersaturation of I_{Si} co-precipitation of O_i and C_s may occur. Thus, for the formation of B-microdefects:



The growth of interstitial microdefects results in a significant decrease of the concentration of interstitial atoms of silicon. It creates conditions for precipitations of impurities. In this case the formation of particles of impurity phase is accompanied by the generation of self-interstitial atoms in positions between knots of the lattice. Thus two types of interstitial microdefects are formed: as interstitial congestion (drains for interstitial atoms of silicon) and as impurity precipitates (sources of these atoms).

Therefore, the vacancy-oxygen aggregation occurs in the vacancy-interstitial mode of crystal growth when the oversaturated solid-state solution of vacancies is decomposed and the vacancy-carbon aggregation occurs when the oversaturated solid-state solution of intrinsic silicon interstitials is decomposed. At a certain critical value of V/G ratio both independent mechanisms (vacancy-type and interstitial-type) result in generation of D-microdefects. These D-microdefects are uniform distributed small-size B-microdefects, which are further transformed into A-microdefects. At the interstitial-type crystal growth mode the growth of precipitates facilitate the oversaturation in self-interstitials and induce the homogeneous nucleation of interstitial clusters (interstitial-type dislocation loops, i.e. A-microdefects). In general, A-microdefects are formed during B-microdefect transformation both through the mechanism of prismatic extruding or through the condensation of silicon intrinsic interstitials.

For vacancy-type mechanism:

- 1) $nO_i + V_{Si} \rightarrow n(VO_2) \rightarrow \text{vacancy-type microdefects}.$
- 2) $n(VO_2) + O_i + \dots + nO_i \rightarrow n[(V_n O_n) + I_{Si}] \rightarrow \text{D-microdefects}.$

For interstitial-type mechanism:

- 1) $C_s + I_{Si} \rightarrow (C_s I_{Si}) \rightarrow \text{D-microdefects}.$
- 2) $(C_s I_{Si}) + O_i \rightarrow n[(C_s I_{Si}) + O_i] \rightarrow \text{B-microdefects}.$
- 3) $\text{B-microdefects} + I_{Si} \rightarrow \text{A-microdefects}.$

Thus, follows that regardless of the growth method of dislocation-free silicon single-crystals, the interstitial-type and vacancy-type microdefects are arisen during the crystals cooling below the temperature of crystallization, and then transformed into interstitial-type microdefects. Further transformation of interstitial-type microdefects follows the scheme: D-microdefects \rightarrow B-microdefects \rightarrow A-microdefects. When the oversaturated solid-state solution of intrinsic point defects is decomposed the background oxygen and carbon impurities present themselves as nucleation centers of grown-in microdefects and participate in their further growth and transformation.

We consider the suggested mechanism as the "core" of formation mechanism of defects. To change the "core" (i.e. to control decomposition of the oversaturated solid solutions of point defects) is possible as follows:

- to vary thermal growth conditions (growth rate, temperature gradients at the phase boundary, cooling rate);
- to adjust the condition of the native point defects ensemble in the crystal by employing various external factors (doping, radiation, etc.);
- to subject the grown single crystals to different kinds of thermal processing.

The heterogeneous mechanism of grown-in microdefects formation describes in the whole the defect structure of small-scale FZ-Si and CZ-Si crystals. From our viewpoint this heterogeneous mechanism works in case of large-scale crystals FZ-Si and CZ-Si. Although new type of grown-in microdefects, namely vacancy microvoids, appear in such crystals. We believe the vacancy microvoids are as secondary defects as A-microdefects. They appear due to change in growth conditions for large-scale FZ-Si and CZ-Si crystals.

3.2 Grown-in microdefects in large-diameter silicon crystals. In small-scale crystals under changing thermal growth conditions the grown-in microdefects of any type except for microvoids are appeared. Adjusting the thermal growth conditions in large-scale crystals shows that dislocation-free growth is available within the limited range of growth rate. From Fig. 6 one can see that above is existence conditions for ring of D(C)-microdefects (often called as ring OSF-defects), for A-microdefects outside the ring of D(C)-microdefects and for (I+V)-microdefects inside the ring of D(C)-microdefects.

Recently the authors [61] have used the X-ray diffuse scattering method to detect both interstitial-type and vacancy-type defects coexisting at CZ-Si vacancy-interstitial-type growth. This experimental results reveal that in large-scale CZ-Si the cooling-induced decomposition of the oversaturated solid solution of point defects follows two mechanisms: vacancy-type and interstitial-type. Then why do microvoids appear in large-scale crystals, but not in small-scale crystals?

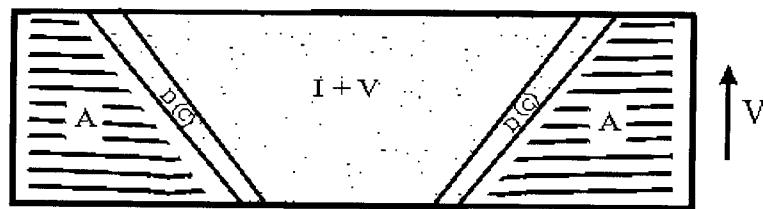


Fig. 6. Schematic image large-diameter silicon crystals, plane (112).

It was defined that microvoids are forming and growing at the temperature range ~ 1100 to 1070°C and the oxide film on their side-walls is growing at the temperature range $\sim 1050 \dots 900^\circ\text{C}$ [62-64]. Here, microvoids have been forming in the large-diameter crystals under conditions of vacancy-interstitial-type growth, which is characterized by relatively fast growth rates, lesser curvature of crystallization front and a small temperature gradient. Under such growth conditions, at a certain cooling stage as thermal conditions change it is quite possible that the pure vacancy agglomeration will prevail over oxygen-vacancy one. Vacancy agglomeration will result in forming single or dual-type microvoids and their thermodynamic equilibrium shape will be octahedral [14]. As is well-known, single microvoids are formed under a relatively rapid cooling rate and a small oxygen concentration, and dual-type microvoids are formed under a relatively slow cooling rate and a large oxygen concentration while the oxide film is growing on side-walls of microvoids and hinders further growth of dual microvoids [64].

As established by [62], short-time thermal processing (during from 15 minutes at $T = 1100^\circ\text{C}$) induces microvoids to diminish their size steeply and to change the structure and, what is more important, precipitates are revealed. It is determined, that small voids are first to diminish and disappear and then large voids of dual microvoids [62]. Thorough observations make it clear that the process of microvoid size diminishing begins in the area between two voids [64]. Hence, the process of the microvoid formation runs at the expense of the process of vacancy agglomeration on

the nucleation centers during crystal cooling. Nucleation centers may be either agglomerates of oxygen-vacancy type or agglomerates of carbon-interstitial type that are formed at higher temperatures. Under certain thermal growth conditions of large-scale silicon crystals the vacancy oversaturation becomes a prevailing factor to precipitate vacancies on oxygen-vacancy and carbon-interstitial aggregates. Above assertion is verified by the experimental fact that there is an oxygen in certain microvoids and a carbon in other microvoids [65]. Paper [62] is a direct support to the heterogeneous formation mechanism of grown-in microdefects in large-scale crystals [4]. Therefore, we may establish a fact that octahedral microvoids and interstitial-type A-microdefects are secondary defects.

3.3. Physical classification of the grown-in microdefects. Silicon single crystals contain a noticeable number of growth impurities (doping or background) that engender the complex systems like “semiconductor-impurity” to be created in crystals. Under certain conditions (temperature, impurity concentration) such systems become the decomposing solid solutions. As their intrinsic point defects not having drains, the impurities are actively involved in the decomposition of solid solution of the point defects. As is seen from experimental results of our study the main and determining factor when the decomposition of solid solution of the point defects in semiconductor silicon concerned is the formation of primary defects either in the form of oxygen-vacancy aggregates (identified here as SiO_2 microprecipitates) or carbon-interstitial aggregates (identified here as SiC micro-precipitates). Heterogeneous nature of defects nucleation determines in substance the further defect formation mechanism in semiconductor silicon.

As effective drains in the form of dislocations are not available, the decomposition of solid solution of the point defects entails the intensive formation of structure from secondary strains, which are agglomerates of intrinsic point defects. Nature of secondary defects is established by low equilibrium density of the intrinsic point defects as well as by the value and sign of the misfit volume, which accompany the formation of new phase. Consequently, the decomposition of solid solution of the point defects is first and foremost distinguished for the generation of secondary defects when the new phase particle is growing. The generation is defined by the atom volume difference between the matrix and precipitate. At that, the secondary defects are mostly localized as agglomerates close to precipitates.

As our study of hyper pure CZ-Si and FZ-Si crystals shows the secondary defects revealed in them are interstitial-type A-microdefects (interstitial dislocation loops) and vacancy-type octahedral microvoids. Consequently, the lattice imperfection can be defined by not only new phase particles having insignificant total volume due to low impurity solubility in silicon, but by secondary defects. They diffuse to a distance of few micrometers from the new phase particles that generated them, spread over the total volume of crystal and make a problem for its use in future.

Primary and secondary grown-in microdefects existing in silicon single crystals gives us an opportunity to introduce a new classification. Such a classification must include all known grown-in microdefects and proceed from the kinematics of defect formation which is defined by the heterogeneous formation mechanism of the microdefects. From our point of view, such classification may avoid discrepancy in letter designations and concepts that constitute a problem in understanding the grown-in microdefects in dislocation-free silicon, which originates from existing practice to assign a letter designation to a microdefect of a certain type. At the same time a classification must reveal the physical nature of defect formation and be simple and coherent.

So, on the basis of heterogeneous formation mechanism of the grown-in microdefects and introduced concepts of primary and secondary grown-in microdefects we may develop a new physical classification (Fig. 7). It follows from the assumption that the primary oxygen-vacancy and carbon-interstitial agglomerates formed on impurity centers are the motive force of defect formation. Under certain thermal conditions of crystal growth the process of defect formation entails

the generation of secondary defects (agglomerates of intrinsic point defects). In this case the oxygen-vacancy and carbon-interstitial agglomerates (B-, D- and I+V-microdefects) turn to be the primary grown-in microdefects and the agglomerates of intrinsic point defects turn to be the secondary grown-in microdefects (A-microdefects and vacancy microvoids). To form some type of grown-in microdefects or other it depends on adjusting the thermal conditions of crystal growth. We think this classification is simple and reflects the physical nature of the defect formation mechanism in dislocation-free silicon single crystals. Fig. 7 outlines the physical classification posed as described above.

In addition to the physical classification, Fig. 7 depicts the universal heterogeneous formation mechanism of the grown-in microdefects in semiconductor silicon crystals of different diameters. Recombination of intrinsic point defects at about crystallization temperature is hindered because of recombination barrier. Cooling-induced decomposition of the oversaturated solid solution of point defects in silicon follows two mechanisms: vacancy-type and interstitial-type. Background impurities of oxygen and carbon are involved in the process of defect formation as nucleation centers, and consequently participate in the processes of further growth and transformation of the grown-in microdefects. As nucleation centers for oxygen-vacancy aggregates serve the areas of contraction close to oxygen interstitial atoms, the redundant vacancies and other oxygen interstitial atoms are directed towards them. As nucleation centers for carbon-interstitial aggregates serve the areas of strain around of carbon substitutions, the redundant intrinsic interstitial atoms and oxygen interstitial atoms are directed towards them. Such agglomerates growth results in the formation of (I+V)-microdefects. The latter are primary microdefects, which are formed near the crystallization front. However, V-microdefects are not referred to microvoids. They are oxygen-vacancy agglomerates (SiO_2 microprecipitates). Growth and transformation of (I+V)-microdefects gives rise to formation of the secondary defects (A-microdefects) [16]. In real small-scale crystals the microvoids are not formed.

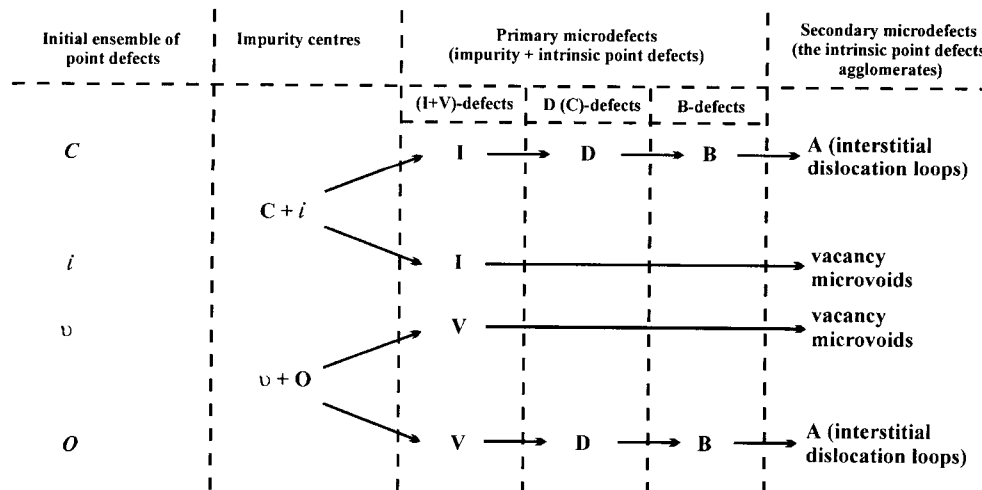


Fig. 7. Schematic illustration (physical classification) of the grown-in microdefects based on the heterogeneous mechanism of their formation and transformation: I – interstitial-type agglomerates, V – vacancy-type agglomerates; C – carbon, O – oxygen, i – self-interstitials, v – vacancies

Increasing the crystal diameter leads to an abrupt change of thermal growth conditions as compared to small-scale crystals. Adjusting thermal growth conditions as well as crystal doping allow controlling the formation mechanism and growth of vacancy-type and interstitial-type defects

under conditions of vacancy-interstitial-type growth. This results in the defect size and shape change and give an advantage to vacancy agglomeration over oxygen-vacancy agglomeration. The process leads to the formation of the secondary defects, namely microvoids. Hence, there are secondary defects of two types in large-scale crystals (A-microdefects and microvoids). However, the basic principles (i.e. “core”) of the heterogeneous mechanism suggested for the grown-in microdefects formation in FZ-Si and CZ-Si remain unchanged.

Above mechanism is alternative to assumptions of Voronkov while not denying the importance of V/G ratio and mathematical tool of Voronkov’s model. V/G ratio characterizes the conditions when vacancy microdefects appear (disappear). But non-critical approach to the Voronkov’s model leads to that the “elephants” (A-microdefects and microvoids) can hide the genuine cause and distort the physical nature of the defect formation in dislocation-free silicon single crystals.

3.4. Formation mechanisms of the secondary grown-in microdefects. By the formation mechanism the defects can be divided into two groups: strain-type and coagulation-type. To the strain-type secondary defects we can refer the dislocation loops. They are formed by the prismatic punching-out that is a rather common mechanism of defect generation, which activates under a large difference between the precipitate atomic volume and matrix atomic volume and is independent of its sign. To the coagulation-type secondary defects we can refer the defects of two types. The defects of first type in the form of complete interstitial dislocation loops appear by way of combining the redundant silicon interstitial atoms located near the precipitates into clusters predominantly in directions $\{111\}$ and $\{110\}$. We can suggest that the coagulation mechanism of the secondary defects generation activates at relatively small strain levels near the precipitates when the value of elastic strain is insufficient to induce the shear dislocation loop. The motive force for such secondary defects to grow may be undersaturation with vacancies that gone to relieve the elastic strain near the precipitates. Contrary to above defects the motive force for secondary defects of other type is oversaturation with vacancies. The oversaturation results in generating the single and dual-type octahedral voids near the precipitates.

Low growth rates for a crystal of certain diameter combined with a large curvature of crystallization front and a large axial temperature gradient are crucial parameters affecting the formation of interstitial dislocation loops (A-microdefects) by employing the strain and coagulation mechanisms of the secondary defects formation. At the same time high growth rates for a crystal of certain diameter combined with a small curvature of crystallization front and a small axial temperature gradient bring out to the formation of octahedral microvoids by employing the coagulation formation mechanism of the secondary defects. In view of that during further high-temperature processing the dislocation loops tend to continue to grow, the silicon crystals should be grown under vacancy-interstitial mode because the defect structure at this growth stage is very much controlled either by adjusting the thermal growth conditions or by doping with special dopant impurity (nitrogen, hydrogen) and additional thermal processing. So, as the formation of the microdefect of any type is connected with carbon and oxygen impurities, which are present in the crystal, and also with varying the crystal growth conditions, it is worthwhile to notice that the defect formation may be affected both by selecting the optimal thermal conditions of growth and by improving the quality of raw material for silicon single crystals.

To conclude it should be denoted that the heterogeneous formation mechanism of the grown-in microdefects make it possible to explain the experimental results observed during the microdefect study of dislocation-free silicon single crystals, in particular, how the striated distribution of A- and B-microdefect is generated and suppressed, how impurities affect the nucleation and growth processes of interstitial and vacancy-type microdefects, and thermal growth conditions of the microdefects formation [66]. It is arguable that such a mechanism reflects as complete as possible

the processes that take place in dislocation-free silicon single crystals during the crystal growth and cooling. Results of numerous experiments prove this to be correct.

Conclusion

1. It is established and proved experimentally the heterogeneous formation and transformation mechanism of the grown-in microdefects in dislocation-free silicon single crystals, which use completely new approaches:

- concentrations of vacancies and intrinsic interstitial silicon atoms at the crystallization front near the melting point are comparable, recombination of intrinsic defects are hindered at high temperatures;
- the decomposition of the oversaturated solid-state solution of point defects during the silicon cooling below the crystallization temperature follows two independent mechanisms: vacancy-type and interstitial-type;
- the driving force of the defect formation is initial oxygen-vacancy agglomerates and carbon-interstitial agglomerates formed on impurities centers;
- the reigning feature of decomposition of the oversaturated solid-state solution of point defects is the generation of secondary defects (agglomerates of intrinsic point defects), which accompanies a new phase growth (the primary defects).

2. At a certain thermal growth conditions the aggregation of point defects under vacancy-interstitial-type or interstitial type growth mode in the course of crystal cooling may cause the secondary defects occurrence around primary oxygen-vacancy and carbon-interstitial aggregates, namely vacancy octahedral microvoids and interstitial-type dislocation loops, accordingly.

3. The physical classification of grown-in microdefects based on the heterogeneous mechanism of grown-in microdefects formation in semiconductor silicon is proposed.

Acknowledgements. The authors are want to thank Dr. M. Ya. Dashevskii (MISA, Russia) for useful discussion of our results and support's.

Literature References

- [1] T. Abe, T. Samizo and S. Marujama: *Jpn. J. Appl. Phys.* Vol. 5 (1966), p. 458.
- [2] A.J.R. de Kock: *J. Electrochem. Soc.* Vol. 118 (1971), p. 1851.
- [3] A.J.R. de Kock, P.J. Roksnoer and P.G.T. Boonen: *J. Cryst. Growth* Vol. 22 (1974), p. 311.
- [4] V.I. Talanin, I.E. Talanin and D.I. Levinzon: *Cryst. Res. & Technol.* Vol. 37 (2002), p. 983.
- [5] L.J. Bernewitz, B.O. Kolbesen, K.R. Mayer and G.E. Shuh: *Appl. Phys. Lett.* Vol. 25 (1974), p. 277.
- [6] B.O. Kolbesen and A. Muhlbauer: *Sol. State Electr.* Vol. 25 (1977), p. 1561.
- [7] H. Foll, V. Gosele and B.O. Kolbesen: *J. Cryst. Growth* Vol. 40 (1977), p. 90.
- [8] A. Bourret, J. Thibault-Desseaux and D.N. Seidman: *J. Appl. Phys.* Vol. 55 (1984), p. 825.
- [9] V.V. Voronkov and M.G. Milvidskii: *Kristallographya* Vol. 33 (1988), p. 471.
- [10] N.V. Veselovskaya, E.G. Sheikhet, K.N. Neimark and E.S. Falkevich: *Rost i legirovanie polyprovodnikovych kristallov i plenok*. Vol. 2 (Nauka Russia 1977), p. 284.
- [11] A.J.R. de Kock, W.T. Stacy and W.M. van de Wijgert: *Appl. Phys. Lett.* Vol. 34 (1979), p. 611.
- [12] A.J.R. de Kock and W.M. van de Wijgert: *J. Cryst. Growth* Vol. 49 (1980), p. 718.
- [13] P.J. Roksnoer and M.M.B. van den Boom: *J. Cryst. Growth* Vol. 53 (1981), p. 563.

-
- [14] V.V. Voronkov: *J. Cryst. Growth* Vol. 59 (1982), p. 625.
- [15] A.A. Sitnikova, L.M. Sorokin, I.E. Talanin, E.G. Sheikhet and E.S. Falkevich: *Phys. Stat. Sol. (a)*. Vol. 90 (1985), p. K31.
- [16] V.I. Talanin, I.E. Talanin and D.I. Levinzon: *Semicond. Sci. & Technol.* Vol. 17 (2002), p. 104.
- [17] H. Shimizu, C. Munakata, N. Honma, S. Aoki and Y. Kosaka: *Jpn. J. Appl. Phys.* Vol. 31 (1992), p. 1817.
- [18] K. Harada, H. Tanaka, T. Watanabe and H. Furuya: *Jpn. J. Appl. Phys.* Vol. 37 (1998), p. 3194.
- [19] S. Sadamitsu, S. Umeno, Y. Koike, M. Hourai, S. Sumita and T. Shigematsu: *Jpn. J. Appl. Phys.* Vol. 32 (1993), p. 3675.
- [20] W. von Ammon, E. Dornberger and P.O. Hansson: *J. Cryst. Growth* Vol. 198-199 (1999), p. 390.
- [21] J. Furukawa, H. Tanaka, Y. Nakada, N. Ono and S. Shiraki: *J. Cryst. Growth* Vol. 210 (2000), p. 26.
- [22] N.I. Puzanov and A.M. Eidenzon: *J. Cryst. Growth* Vol. 137 (1994), p. 642.
- [23] S. Umeno, Y. Yanase, M. Hourai, M. Sano, Y. Shida and H. Tsuya: *Jpn. J. Appl. Phys.* Vol. 38 (1999), p. 5725.
- [24] S. Umeno, M. Okui, M. Hourai, M. Sano and H. Tsuya: *Jpn. J. Appl. Phys.* Vol. 36 (1997), p. L591.
- [25] M. Kato, T. Yoshida, Y. Ikeda and Y. Kitagawara: *Jpn. J. Appl. Phys.* Vol. 35 (1996), p. 5597.
- [26] M. Nishimura, S. Yoshino, H. Motoura, S. Shimura, T. Mchedlidze and T. Hikone: *J. Electrochem. Soc.* Vol. 143 (1996), p. L243.
- [27] V.V. Voronkov and R. Falster: *J. Cryst. Growth* Vol. 194 (1998), p. 76.
- [28] V.V. Voronkov and R. Falster: *J. Cryst. Growth* Vol. 198-199 (1999), p. 399.
- [29] P.M. Petroff and A.J.R. de Kock: *J. Cryst. Growth* Vol. 30 (1975), p. 117.
- [30] J. Chikawa and S. Shirai: *J. Cryst. Growth* Vol. 39 (1977), p. 328.
- [31] J.A. van Vechten: *Phys. Rev. B* Vol. 17 (1978), p. 3197.
- [32] S.M. Hu: *J. Vac. Sci. and Technol.* Vol. 14 (1977), p. 17.
- [33] E. Sirtl: *Semiconductor silicon*. (Princeton, Electrochem. Soc. 1977), p. 4.
- [34] V.V. Voronkov and R. Falster: *J. Electrochem. Soc.* Vol. 149 (2002), p. G167.
- [35] M. Pasemann and P. Werner: *Phys. Stat. Sol. (a)* Vol. 54 (1979), p. 179.
- [36] M. Pasemann and P. Werner: *Phys. Stat. Sol. (a)* Vol. 58 (1980), p. K1.
- [37] M. Okui and M. Nishimoto: *J. Cryst. Growth* Vol. 237-239 (2002), p. 1651.
- [38] K.V. Ravi and C.J. Varker: *J. Appl. Phys.* Vol. 45 (1974), p. 272.
- [39] K.N. Neimark, B.A. Sakharov, B.F. Chulitskii and M.I. Osovskii: *Kremnii i Germanii*. Vol. 2 (Metallurgia, Russia 1970), p. 32.
- [40] V.I. Talanin and I.E. Talanin: *Phys. Stat. Sol. (a)* Vol. 200 (2003), p. 297.
- [41] M. Wilkens and H. Foll: *Phys. Stat. Sol. (a)* Vol. 49 (1978), p. 555.
- [42] J.B. Mitchell and W.L. Bell: *Acta Met.* Vol. 24 (1976), p. 147.
- [43] A. Seeger, W. Frank and U. Gosele: *Defects and radiation effects in semiconductors*. Vol. 46 (1979), p. 148.
- [44] U. Gosele, W. Frank and A. Seeger: *J. Appl. Phys.* Vol. 23 (1980), p. 361.
- [45] U. Gosele, W. Frank and A. Seeger: *Solid State Commun.* Vol. 45 (1983), p. 31.
- [46] J. Dzelme, I. Ertsinsh, B. Zapol and A. Misiuk: *Phys. Stat. Sol. (a)* Vol. 171 (1999), p. 197.
- [47] L. Fedina, A. Gutakovskii, A. Aseev, J. van Landuyt and J. Vanhellemont: *Phys. Stat. Sol. (a)* Vol. 171 (1999), p. 147.
- [48] L. Fedina, A. Gutakovskii and A. Aseev: *Cryst. Res. & Technol.* Vol. 35 (2000), p. 775.
- [49] R. Tognato: *Phys. Stat. Sol. (a)* Vol. 98 (1986), p. K133.
- [50] S. Pizzini: *Phys. Stat. Sol. (a)* Vol. 171 (1999), p. 123.

- [51] K.H. Katerbau: *Phys. Stat. Sol. (a)* Vol. 38 (1976), p. 463.
- [52] S.M. Ohr: *Phys. Stat. Sol. (a)* Vol. 38 (1976), p. 553.
- [53] A.A. Sitnikova, L.M. Sorokin and E.G. Sheikhet: *Fizika Tverdogo Tela* Vol. 29 (1987), p. 2623.
- [54] T.Y. Tan and W.K. Tice: *Phil. Mag.* Vol. 34 (1976), p. 615.
- [55] H. Bender: *Phys. Stat. Sol. (a)* Vol. 86 (1984), p. 245.
- [56] Y. Matsushita, S. Kishino and M. Kanamori: *Jpn. J. Appl. Phys.* Vol. 19 (1980), p. L101.
- [57] H. Foll and B.O. Kolbesen: *J. Appl. Phys.* Vol. 8 (1975), p. 319.
- [58] A.A. Sitnikova, L.M. Sorokin, I.E. Talanin, K.L. Malyshev, E.G. Sheikhet and E.S. Falkevich: *Fizika Tverdogo Tela* Vol. 28 (1986), p. 1829.
- [59] H. Foll and M. Wilkens: *Phys. Stat. Sol. (a)* Vol. 31 (1975), p. 519.
- [60] S. Iida, Y. Aoki, Y. Sugita, T. Abe and H. Kawata: *Jpn. J. Appl. Phys.* Vol. 39 (2000), p. 6130.
- [61] V.T. Byblik and N.M. Zotov: *Kristallographya* Vol. 42 (1997), p. 1103.
- [62] M. Itsumi: *J. Cryst. Growth* Vol. 237-239 (2002), p. 1773.
- [63] Y. Yanase, H. Nishihata, T. Ochiai and H. Tsuya: *Jpn. J. Appl. Phys.* Vol. 37 (1998), p. 1.
- [64] T. Ueki, M. Itsumi, T. Takeda, K. Yoshida, A. Takaoka and S. Nakajima: *Jpn. J. Appl. Phys.* Vol. 37 (1998), p. L771.
- [65] T. Ueki, M. Itsumi and T. Takeda: *Jpn. J. Appl. Phys.* Vol. 38 (1999), p. 5695.
- [66] V.I. Talanin, I.E. Talanin and D.I. Levinzon: *Crystallography Reports* Vol. 49 (2004), p. 188.